

---

This is an electronic reprint of the original article.  
This reprint may differ from the original in pagination and typographic detail.

Lehrhofer, Anna F.; Fliri, Lukas; Bacher, Markus; Budischowsky, David; Sulaeva, Irina; Hummel, Michael; Rosenau, Thomas; Hettegger, Hubert

## **A mechanistic study on the alleged cellulose cross-linking system: Maleic acid/sodium hypophosphite**

*Published in:*  
Carbohydrate Polymers

*DOI:*  
[10.1016/j.carbpol.2024.122653](https://doi.org/10.1016/j.carbpol.2024.122653)

Published: 15/12/2024

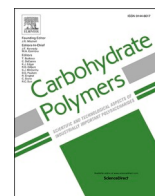
*Document Version*  
Publisher's PDF, also known as Version of record

*Published under the following license:*  
CC BY

*Please cite the original version:*  
Lehrhofer, A. F., Fliri, L., Bacher, M., Budischowsky, D., Sulaeva, I., Hummel, M., Rosenau, T., & Hettegger, H. (2024). A mechanistic study on the alleged cellulose cross-linking system: Maleic acid/sodium hypophosphite. *Carbohydrate Polymers*, 346, Article 122653. <https://doi.org/10.1016/j.carbpol.2024.122653>

---

This material is protected by copyright and other intellectual property rights, and duplication or sale of all or part of any of the repository collections is not permitted, except that material may be duplicated by you for your research use or educational purposes in electronic or print form. You must obtain permission for any other use. Electronic or print copies may not be offered, whether for sale or otherwise to anyone who is not an authorised user.



# A mechanistic study on the alleged cellulose cross-linking system: Maleic acid/sodium hypophosphite

Anna F. Lehrhofer<sup>a</sup>, Lukas Fliri<sup>b</sup>, Markus Bacher<sup>a</sup>, David Budischowsky<sup>a</sup>, Irina Sulaeva<sup>a,c</sup>, Michael Hummel<sup>b</sup>, Thomas Rosenau<sup>a,d,\*</sup>, Hubert Hettegger<sup>a,e,\*</sup>

<sup>a</sup> Institute of Chemistry of Renewable Resources, Department of Chemistry, University of Natural Resources and Life Sciences, Vienna (BOKU), Muthgasse 18, A-1190 Vienna, Austria

<sup>b</sup> Department of Bioproducts and Biosystems, Aalto University, P.O. Box 16300, 0076 Aalto, Finland

<sup>c</sup> Core Facility Analysis of Lignocellulosics (ALICE), University of Natural Resources and Life Sciences, Vienna (BOKU), Konrad-Lorenz-Strasse 24, A-3430 Tulln, Austria

<sup>d</sup> Laboratory of Natural Materials Technology, Faculty of Science and Engineering, Åbo Akademi University, Porthansgatan 3, 20500 Turku, Finland

<sup>e</sup> Christian Doppler Laboratory for Cellulose High-Tech Materials, University of Natural Resources and Life Sciences, Vienna (BOKU), Konrad-Lorenz-Strasse 24, A-3430 Tulln, Austria

## ARTICLE INFO

### Keywords:

Cellulose  
Cross-linking  
Durable press finishing  
Maleic acid  
Sodium hypophosphite  
Textile finishing

## ABSTRACT

A combination of maleic acid and sodium hypophosphite as a durable press finishing agent has been reported as a safer but equally effective alternative to conventional formaldehyde-based cross-linking agents for applications in cellulose-based fiber and textile finishing. However, the mechanistic details of this system have not yet been fully elucidated to allow optimization of the conditions. Effective cross-linking treatment requires high curing temperatures of  $\geq 160$  °C, which enhances oxidative and thermal degradation of cellulose. In this work, the sequential steps of the cross-linking mechanism were investigated both with model compounds and cellulosic substrates. Extensive NMR studies on model compounds revealed several side reactions alongside the synthesis of the targeted cross-linkable moiety. As an alternative, to circumvent side reactions, a two-step procedure was used by synthesizing the cross-linker sodium 2-[(1,2-dicarboxyethyl)phosphinate]succinic acid in a well-defined pre-condensation reaction before application onto the cellulosic substrate. Further, the effect of the cross-linking treatment on the molecular weight distribution of cellulose was studied by gel permeation chromatography, which showed degradation due to maleic acid/sodium hypophosphite treatment. By using sodium 2-[(1,2-dicarboxyethyl)phosphinate]succinic acid and sodium hypophosphite, this degradation could be significantly limited.

## 1. Introduction

Cross-linking of cellulosic fibers is a technique used to conveniently alter the material properties for specific textile applications. For example, wrinkle performance, fibrillation resistance, and fire retardancy can be notably improved (Zhu & Liu, 2018; Liu et al., 2019; Ma, Rissanen, et al., 2021). At present, formaldehyde and/or amino-based cross-linking agents are still applied as durable press finishing agents, such as 1,3,5-triacryloylhexahydro-1,3,5-triazine (TAHT) and dimethyloldihydroxyethyleneurea (DMDHEU) (Ma, You, et al., 2021). Although they enhance the textiles' overall performance, the toxicity of these

chemicals remains a major concern. While TAHT synthesis involves formaldehyde as a reactant, DMDHEU is essentially formed by a mixture of formaldehyde, glyoxal, and urea in an equilibrium reaction. In both cases, this can lead to the release of toxic and cancerogenic formaldehyde from the cross-linked fibers (Liu et al., 2016; Ma, You, et al., 2021). Consequently, the replacement of these traditional cross-linking agents has been a major target over the last decades to address ecological and health concerns (Wang et al., 2023).

The use of poly(carboxylic acids) (PCAs) as a more ecological and less toxic alternative perhaps represents the most promising and best-studied substitute in this regard. Mechanistically, cross-linking of

\* Corresponding authors at: Institute of Chemistry of Renewable Resources, Department of Chemistry, University of Natural Resources and Life Sciences, Vienna (BOKU), Muthgasse 18, A-1190 Vienna, Austria.

E-mail addresses: [anna.lehrhofer@boku.ac.at](mailto:anna.lehrhofer@boku.ac.at) (A.F. Lehrhofer), [lukas.fliri@aalto.fi](mailto:lukas.fliri@aalto.fi) (L. Fliri), [markus.bacher@boku.ac.at](mailto:markus.bacher@boku.ac.at) (M. Bacher), [david.budischowsky@boku.ac.at](mailto:david.budischowsky@boku.ac.at) (D. Budischowsky), [irina.sulaeva@boku.ac.at](mailto:irina.sulaeva@boku.ac.at) (I. Sulaeva), [michael.hummel@aalto.fi](mailto:michael.hummel@aalto.fi) (M. Hummel), [thomas.rosenau@boku.ac.at](mailto:thomas.rosenau@boku.ac.at) (T. Rosenau), [hubert.hettegger@boku.ac.at](mailto:hubert.hettegger@boku.ac.at) (H. Hettegger).

<https://doi.org/10.1016/j.carbpol.2024.122653>

Received 29 May 2024; Received in revised form 24 July 2024; Accepted 22 August 2024

Available online 23 August 2024

0144-8617/© 2024 The Authors. Published by Elsevier Ltd. This is an open access article under the CC BY license (<http://creativecommons.org/licenses/by/4.0/>).

cellulose chains by PCAs proceeds in two steps: An activated, five-membered cyclic anhydride is formed by intramolecular condensation of two vicinal carboxylic acid groups before it reacts with free cellulosic hydroxy groups in an esterification reaction. Therefore, at least three vicinal carboxylic acid groups (e.g., citric acid), or two pairs of vicinal carboxylic acids on one single cross-linker molecule are needed for efficient reaction (Hu et al., 2022; Mao & Yang, 2001a). 1,2,3,4-Butanetetracarboxylic acid (BTCA) is a highly effective cross-linking agent, but also more costly than traditional cross-linking agents or other PCAs. Citric acid (CA) as a natural PCA with three carboxylic acid moieties is non-toxic and inexpensive, however, it is less effective and can induce significant yellowing in treated fibers (Ma, You, et al., 2021; Yao et al., 2013).

Dicarboxylic acids, such as itaconic acid (IA) and maleic acid (MA), can esterify cellulose only once via the formation of an activated anhydride and can thus not cross-link on their own. However, when combined with sodium hypophosphite (SHP) as an additional reactant, they significantly improve fabric properties (Mao & Yang, 2001b; Peng, Yang, & Wang, 2012; Peng, Yang, Wang, & Wang, 2012; Wang et al., 2023). MA/SHP-treated fibers showed improved wrinkle resistance, in a range comparable to DMDHEU-modified samples, while retaining higher fabric strength. Moreover, due to the incorporation of phosphorus, the materials exhibited enhanced fire retardancy (Granzow, 1978), making this cost-efficient system especially interesting for industrial applications (Peng, Yang, & Wang, 2012). Consequently, the MA/SHP treatment has been increasingly used and empirically optimized towards improved curing conditions and an ideal (molar) ratio of the reagents. Experiments substituting MA with succinic acid (SA) or SHP with phosphite indicated that a reaction between two C=C bonds and the H-P-H unit of the hypophosphite molecule was supposed to cause the covalent cross-linking (Peng, Yang, & Wang, 2012). Although there is no definite experimental proof to date, literature reports refer to essentially three consecutive mechanistic steps (Fig. 1): 1) the esterification of cellulose by MA via the activated anhydride; 2) the addition of the first P-H bond of the hypophosphite to the double bond of the MA ester (i.e., hydrophosphinylation); and 3) the actual cross-linking reaction by the addition of the second P-H bond of the same SHP moiety to the double bond of another MA ester (Peng, Yang, & Wang, 2012; Yang et al., 2010, 2011).

Esterification via an intermediate anhydride is likely to proceed as the initial step, as temperatures of only 100–130 °C are needed. Several studies attribute a bifunctional role to SHP. They state that SHP does not only form a part of the cross-linker itself but also aids esterification as a

catalyst (Yang et al., 2010; Ji et al., 2015, Ji et al., 2016). In the subsequent hydrophosphinylation, a minimum curing temperature of around 160–170 °C is needed for efficient cross-linking. At this temperature and above, increasing wrinkle recovery angles (WRA) and higher phosphorus contents were measured, assuming cross-link formation according to Fig. 1 (Peng, Yang, & Wang, 2012; Yang et al., 2010). In literature reports, enhanced WRA and fibrillation resistance of cellulosic materials are often directly attributed to covalent cross-linking between the fibers. However, this cross-linking is in fact very challenging to prove on the molecular level, as durable press finishing treatment commonly goes hand in hand with decreased solubility of the substrate and thereby significantly limits the applicability of analytical methods. Thus, questions arise if the altered properties are due to intramolecular, covalent cross-links, other chemical reactions between cellulose and the finishing reagents (such as hydrophobization), or whether they could rather be attributed to physical phenomena.

Since, from the mechanistic perspective, (transition)metal-catalyzed or radical-initiator mediated routes have been reported for hydrophosphinylation (Huang et al., 2022; Markoulides & Regan, 2012; Montchamp, 2005, 2014; Ortial et al., 2013; Parsons & Wright, 2008; Platten et al., 2022), the addition of SHP to MA under the prevailing conditions is likely to proceed via a radical pathway. Owing to the high curing temperature, unwanted side reactions of the highly reactive radical species can be expected, which might initiate cellulose degradation. Furthermore, phosphorus-containing species are prone to undergo various reactions, such as disproportionation or other redox reactions due to the various possible oxidation states (Liu et al., 2017). Besides affecting cellulose integrity, such processes might also generate highly toxic organo-phosphorus compounds, some of which are commonly known as pesticides or even neurotoxins (Davis et al., 1985; O'Brien, 2013). Consequently, it is advisable to avoid such reaction conditions due to both environmental and possible health concerns. Thus, the synthesis of a PCA-based cross-linker in a defined, catalyzed reaction prior to the actual application onto the cellulosic material appears to represent a better alternative that gives improved control of the cross-linking process.

Chen and co-workers obtained polymaleic acid (PMA) from radical Na<sub>2</sub>S<sub>2</sub>O<sub>8</sub>-mediated polymerization of MA and SHP and applied it as a durable press finishing agent. Treated fabrics showed a WRA similar to DMDHEU- and BTCA-cross-linked samples while retaining higher tensile strength. Further, PMA is formaldehyde-free, more cost-efficient, and causes no yellowing of the treated fabrics (Chen et al., 2005; Cheng & Yang, 2009). Similar procedures are also found in the patent literature,

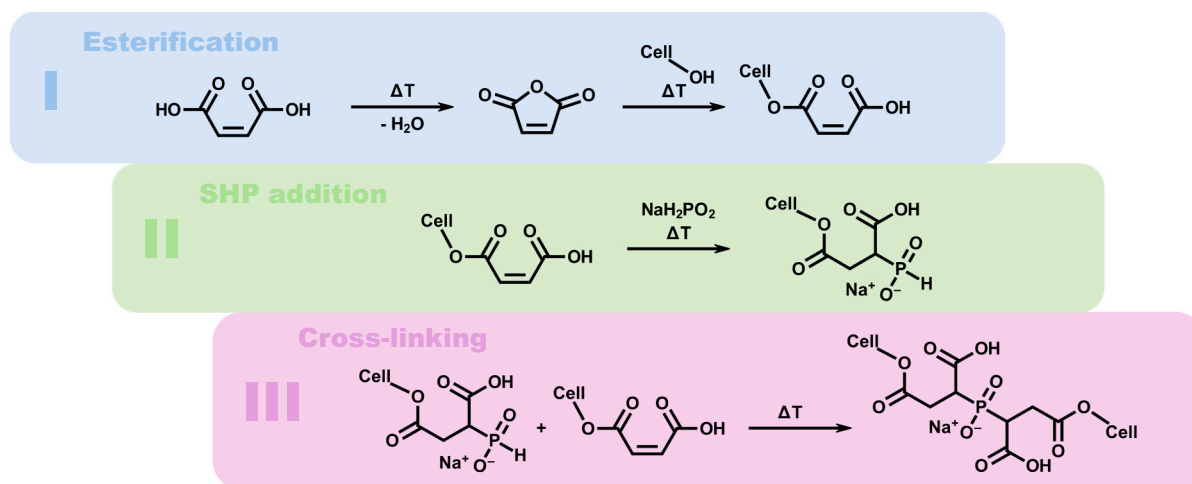


Fig. 1. Cross-linking mechanism of MA/SHP suggested in the literature, proceeding in essentially three consecutive steps: I) Esterification of cellulose (Cell) via formation of the activated MAH; II) First addition of SHP to the C=C bond of esterified MA; III) Cross-linking by second addition of the same SHP moiety to another MA cellulose ester (Peng, Yang, & Wang, 2012; Yang et al., 2010).

where a mixture of oligomeric MA in combination with SHP is described (Gardner et al., 2006; Sivik et al., 2007). Compared to Chen and co-workers, a comparably lower MW of the PMA is achieved by (partial) deprotonation of MA prior to condensation. Similar results were obtained by a low-molecular-weight product synthesized by copolymerization of MA, acrylic acid (AA), and SHP (Liang et al., 2020). Yet, the structures of these oligomeric cross-linkers have not been unambiguously elucidated, as no defined, neat compounds were isolated, but the product mixtures were directly used for fabric treatment. By implementing an acid-catalyzed thiol-ene click reaction with MA and 1,2-dimercaptoethane, Hu and co-workers synthesized a well-defined cross-linker with four carboxylate moieties, ethyldimercaptan disuccinic acid (EDMDSA), which exhibited slightly lower WRA than BTCA, but significantly better strength retention due to its flexible backbone structure (Hu et al., 2022). Thus, the approach provided better control of the mechanism and the formation of cross-links.

In summary, successful applications of the MA/SHP system were described in the literature for both the direct exposure of cellulosic fibers to aqueous solutions containing the educts, or the sequential approach relying on the step-wise, separate synthesis of the cross-linking moiety. From an industrial perspective, the simpler one-pot approach seems preferable. However, given the complex and not yet sufficiently understood reactions, involving temperatures up to 180 °C, the occurrence of side reactions seems to be an unsolved problem. These side reactions and the resulting byproduct formation can in turn result in consequences regarding the material properties or give rise to eco-toxicological concerns.

In the study at hand, it was attempted to further elucidate the underlying reaction mechanisms in the MA/SHP cross-linking treatment and to shed light on the occurring side reactions to provide a solid base for further discussions and an improved, targeted application of this cross-linking system. For this endeavor, the individual steps of the hypothesized mechanism were investigated using small-molecular model compounds and solution-state NMR screenings. The influence of the MA/SHP cross-linking treatment on cellulose degradation was studied by gel permeation chromatography (GPC-MALLS-RI). Additionally, the cross-linking agent 2-[(1,2-dicarboxyethyl)phosphinate]succinic acid (compound 1) was selectively synthesized using a pre-condensation approach similar to patent literature (Sivik et al., 2007). The obtained compounds and intermediates were thoroughly characterized and tests concerning the reactivity towards cellulose were conducted. Further, we aimed to compare the traditional one-pot approach to the alternative pre-condensation approach with regard to the side reactions and cellulose degradation.

## 2. Materials and methods

### 2.1. Materials and chemicals

Microcrystalline cellulose (Avicel® PH-101, MCC), maleic acid (MA), maleic anhydride (MAH), sodium hypophosphite (SHP), and sodium peroxodisulfate (SPDS) were purchased from Sigma-Aldrich/Merck KGaA (Schnellendorf, Germany) in the highest available purity grade and used without further purification. Deionized water was used for all aqueous solutions. Solvents were purchased in synthesis grade from Roth, Sigma-Aldrich, and VWR International, LLC, and were used as received. Whatman No. 1 paper was obtained from GE Healthcare (production site China) exhibiting a number-average molecular weight ( $M_n$ ) of 180.3 kg/mol, a mass-average molecular weight ( $M_w$ ) of 382.5 kg/mol, a Z-average molecular weight ( $M_z$ ) of 626.6 kg/mol, a dispersity ( $\mathcal{D}$ ) of 2.12 and a carbonyl group content of 0.49  $\mu\text{mol/g}$  measured by GPC-MALLS-RI in DMAc/LiCl using a specific refractive index increment (dn/dc) of 0.140 (Sulaeva et al., 2024).

### 2.2. Methods

Attenuated total reflection Fourier-transformation infrared (ATR-FTIR) spectra were recorded on a Frontier IR single-range spectrometer (PerkinElmer, Waltham, MA, USA) equipped with a diamond/ZnSe crystal, LiTaO<sub>3</sub> detector, and KBr windows. Spectra were obtained and processed using the PerkinElmer Spectrum software (version 10.03.02). Cellulose samples were lyophilized for a minimum of 24 h before the measurement. All spectra were obtained at a spectral range of 4000–600  $\text{cm}^{-1}$ , a spectral resolution of 4  $\text{cm}^{-1}$ , and 16 scans per sample.

Solution-state NMR spectra were recorded using a Bruker Avance II 400 spectrometer equipped with a cryogenically-cooled broadband observing (BBO) 5 mm probe-head (CryoProbe™ Prodigy, N<sub>2</sub>-cooled), or a Bruker Avance III 400 NMR spectrometer equipped with a 5 mm broadband observe (BBFO) probe-head. The NMR experiments were performed with z-gradients at 303 K (unless indicated otherwise) at resonance frequencies of 400.13 MHz for <sup>1</sup>H, 100.61 MHz for <sup>13</sup>C, and 161.98 MHz for <sup>31</sup>P using standard Bruker pulse programs (for more detailed information see SI). Chemical shifts are given in parts per million (ppm) and were referenced to the respective residual solvent signal as internal reference (DMSO-*d*<sub>6</sub>: 2.50 ppm for <sup>1</sup>H, 39.52 ppm for <sup>13</sup>C; D<sub>2</sub>O: 4.79 ppm for <sup>1</sup>H). For all experiments, the number of scans and spectral widths were adjusted individually depending on the nature and the concentration of the sample. Solution-state NMR measurements of cellulosic samples were carried out following a published protocol (Fliri et al., 2023; King et al., 2018; Koso et al., 2020) in [P<sub>4444</sub>][OAc]:DMSO-*d*<sub>6</sub> (1:4 w/w). For the preparation of the NMR samples, the cellulosic material (40 mg) was weighed into a 4 mL glass vial, [P<sub>4444</sub>][OAc]:DMSO-*d*<sub>6</sub> (1:4 w/w) was added until a final weight of 0.80 g, and the sealed vial was stirred at 65 °C overnight. After dissolution, the samples were transferred into standard 5 mm NMR tubes. All spectra were obtained at 338 K. All NMR data were acquired and processed using Bruker TopSpin 3.2.7, 3.6.5, and/or 4.3.0 software.

Gel permeation chromatography (GPC) analysis was performed according to published procedures (Potthast et al., 2015; Siller et al., 2014) using a size exclusion/multi-detector (GPC-MALLS-RI) system. The system was composed of a Bio-Inert 1260 Infinity II HPLC pump (G1312B; Agilent Technologies, Waldbronn, Germany), an HP Series 1100 autosampler (G1367B; Agilent Technologies), MALLS detector (Wyatt Dawn DSP with a diode laser,  $\lambda = 488 \text{ nm}$ , Wyatt Inc.) and refractive index detector (Shodex RI71). Four serial SEC columns (Styragel HMW 6E Mixed Bed, 15–20  $\mu\text{m}$ , 7.8 mm i.d., 300 mm length, Waters GmbH, Vienna, Austria) with one Agilent GPC guard column (PL gel, 20  $\mu\text{m}$ , 7.8 mm i.d., 50 mm length; Agilent Technologies) were used as a stationary phase. As a mobile phase, *N,N*-dimethylacetamide/lithium chloride (0.9 % w/v; filtered through a 0.02  $\mu\text{m}$  filter) was used at a flow rate of 1.0 mL/min. For each measurement, a sample volume of 100  $\mu\text{L}$  was injected at a 45 min run time. The molecular weight distribution (MWD) and its statistical moments were calculated based on a refractive index increment of 0.140 mL/g for cellulose in *N,N*-dimethylacetamide/lithium chloride (0.9 % w/v) at 488 nm. The raw data was processed with Astra 4.73 (Wyatt Technologies) and GRAMS/AI 7.0 software (Thermo Fisher Scientific).

Preparation of cellulose for GPC analysis: Dissolution of pulp samples was carried out according to a published procedure (Potthast et al., 2015). Approximately 12 mg of an air-dried pulp sample was disintegrated using deionized H<sub>2</sub>O and a standard kitchen blender. The suspension was filtered using a Büchner funnel with filter paper (Lab Logistics Group GmbH, Meckenheim, Germany), washed with EtOH, and pre-dried on the filter by vacuum filtration. The sample was transferred into a 4 mL screw-cap vial and activated by shaking in 3 mL DMAc at room temperature for 16–24 h. Subsequently, the sample was filtered and dissolved in 1 mL of DMAc/LiCl (9 % w/v) at room temperature. Prior to analysis, the sample was diluted with pure DMAc (0.3 mL sample solution + 0.9 mL DMAc) and filtered through a 0.45  $\mu\text{m}$  syringe filter.

Experimental details of the LC-ESI-MS analysis can be found in the Supporting Information (section 5).

## 2.3. Syntheses

### 2.3.1. Formation of MAH from MA

MA (10 mg) was placed in a 1.5 mL glass vial and heated to the desired temperature (between 50 and 150 °C) in an ashing furnace (Model No.: LVT 15/11, Nabertherm GmbH, Lilienthal/Bremen, Germany) for a specific time (5 or 60 min). The experiment was repeated with a mixture of MA (10 mg, 86 μmol, 1.0 equiv.) and SHP (7.5 mg, 86 μmol, 1.0 equiv.). The resulting solids were characterized by FTIR and NMR spectroscopy (see **Table S1**, SI).

### 2.3.2. Esterification of 1-octanol with MA and MAH

**2.3.2.1. Temperature study.** MA (0.180 g, 1.55 mmol, 1.0 equiv.) or MAH (0.150 g, 1.54 mmol, 1.0 equiv.) were suspended in 1-octanol (0.26 mL, 0.22 g, 1.7 mmol, 1.1 equiv.) in a 4 mL vial and heated to the desired temperature (50, 75, 100, 125 or 150 °C) in an oil bath for 60 min. The sample was cooled to RT (20 °C) and analyzed by NMR spectroscopy in DMSO-*d*<sub>6</sub>. The yield of the resulting products was determined by integration of the <sup>1</sup>H NMR signals (see **Table S2**, SI).

**2.3.2.2. Monoctyl maleate.** MAH (1.00 g, 10.2 mmol, 1.0 equiv.) was suspended in 1-octanol (1.34 g, 10.1 mmol, 1.01 equiv.) and heated to 60 °C. After 3 h, the solution was cooled to RT and stored in the fridge to allow crystallization. The resulting colorless solid was re-crystallized twice from *n*-hexane (1.80 g, 77 %). <sup>1</sup>H (DMSO-*d*<sub>6</sub>, 400.13 MHz): δ 12.93 (bs, C(O)OH), 6.37 (d, 1H, *J* = 12.0 Hz, CH), 6.33 (d, 1H, *J* = 12.0 Hz, CH), 4.07 (t, 2H, *J* = 7.0 Hz, CH<sub>2</sub>), 1.58 (m, 2H, *J* = 7.0 Hz, CH<sub>2</sub>), 1.25 (m, 12H, 6 × CH<sub>2</sub>), 0.85 (t, 3H, *J* = 7.0 Hz, CH<sub>3</sub>). FTIR (cm<sup>-1</sup>): 2956 (CH), 2921 (CH), 2854 (CH<sub>2</sub>), 1719 (C(O)OR), 1697 (C(O)OH), 1642.

### 2.3.3. Esterification of cellulose

MCC (0.100 g, 0.617 mmol AGU) was placed in a 4 mL vial and 0.50 mL of a MA stock solution in acetone was added (15 mg/mL, 7.5 mg, 0.065 mmol, 0.1 equiv./AGU). The suspension was dried at 75 °C for 20 min and then heated to the desired reaction temperature for 35 min. Subsequently, the sample was cooled to RT, suspended in H<sub>2</sub>O, washed with H<sub>2</sub>O (2×), acetone, and H<sub>2</sub>O (20 mL each), and lyophilized for at least 48 h before further analysis. The reaction was repeated analogously with MAH using an MAH stock solution in acetone (0.50 mL, 13 mg/mL, 0.67 mmol, 0.1 equiv./AGU). The samples were characterized by solution-state NMR spectroscopy according to a published procedure (Fliri et al., 2023).

### 2.3.4. Preparation of sodium 2-[(1,2-dicarboxyethyl)phosphinate]succinic acid (compound 1, structure see Fig. 5)

Maleic acid (3.03 g, 26.1 mmol, 2.02 equiv.) and NaOH (2.18 g, 54.5 mmol, 4.20 equiv.) were dissolved in H<sub>2</sub>O (9.5 mL), sodium hypophosphite (1.14 g, 13.0 mmol, 1.00 equiv.) was added and the colorless suspension was heated to 80 °C in a 20 mL glass vial using an oil bath. Once a clear solution had formed, sodium peroxodisulfate was added in three portions (3 × 0.050 g, 0.63 mmol, 10 mol%) at *t* = 0, 1 and 3 h of reaction time. After 5 h, the solution was cooled to RT and the solvent was evaporated until the sodium salt was obtained as a colorless solid. The product was washed with MeOH (3 × 50 mL) and sonicated in an ultrasonic bath for 10 min to dissolve excess MA. The colorless solid was isolated by filtration, dried, and obtained as the sodium salt in high yield (5.15 g, 97 %, calculated as Na<sub>5</sub>-salt). The product was acidified with HCl (3 M) or H<sub>2</sub>SO<sub>4</sub> (6 M) to pH 1–2 to obtain the tetracarboxylic acid.

**Compound 1 (pH 9, sodium salt):** <sup>1</sup>H (D<sub>2</sub>O, 400.13 MHz): δ 3.32 (m, 1H, CH), 3.15 (m, 1H, CH), 2.71 (m, 2H, CH<sub>2</sub>), 2.52 (m, 2H, CH<sub>2</sub>); <sup>31</sup>P (D<sub>2</sub>O, 161.98 MHz, proton decoupled) δ 34.99 (s), 34.50 (s).

**Compound 1 (pH 1, protonated):** <sup>1</sup>H (D<sub>2</sub>O, 400.13 MHz): δ 3.67 (m, 1H, CH), 3.47 (m, 1H, CH), 3.01 (m, 2H, CH<sub>2</sub>), 2.86 (m, 2H, CH<sub>2</sub>); <sup>31</sup>P{<sup>1</sup>H} (D<sub>2</sub>O, 161.98 MHz, proton-decoupled): δ 27.46 (s), 27.33 (s). <sup>1</sup>H (DMSO-*d*<sub>6</sub>, 400.13 MHz): δ 3.28 (m, 1H, CH), 3.13 (m, 1H, CH), 2.73–2.52 (m, 4H, 2 × CH<sub>2</sub>); <sup>13</sup>C (DMSO-*d*<sub>6</sub>, 100.61 MHz): δ 173.49, 173.35, 173.36, 173.20 (C<sub>q</sub>, C(O)OH), 171.72, 171.68, 171.60, 171.57 (C<sub>q</sub>, C(O)OH), 43.68, 43.66, 42.89, 42.87 (CH), 31.32, 31.31, 30.53, 30.52 (CH<sub>2</sub>). ESI-TOF/MS: *m/z* calcd. for C<sub>8</sub>H<sub>11</sub>O<sub>10</sub>P [M + H]<sup>+</sup> 299.0168, found 299.0163 (± 10 ppm). FTIR (cm<sup>-1</sup>): 1707 (C(O)OH).

### 2.3.5. Esterification of compound 1 with 1-hexanol

In a 4 mL glass vial, compound 1 (protonated, 0.050 g, 0.156 mmol, 1.0 equiv.) was suspended in 1-hexanol (0.155 g, 1.509 mmol, 9.7 equiv.), stirred and heated to 120 °C for 6 h in an oil bath. The resulting slightly yellow solid was lyophilized for 24 h and subsequently analyzed by NMR spectroscopy (for <sup>1</sup>H NMR spectrum and NMR data, see **Fig. S7** in the SI).

### 2.3.6. Preparation of SHP/MA-treated cellulose

Whatman filter paper No. 1 (approximately 100 mg) was dipped into an aqueous solution containing 8 % MA (w/w) and 5 % SHP (w/w) (molar ratio: 1.2/1.0 MA/SHP; pH at 25 °C = 1.62) and padded dry using standard laboratory pulp. The procedure was repeated once until a weight gain of approximately 100 % was reached. The sample was dried at 85 °C for 5 min in a laboratory drying oven and cured at 170 °C (alternatively 180 °C) for 5 min in an ashing furnace. Subsequently, the sample was washed with deionized water (approximately 1 L), disintegrated in a kitchen mixer, filtered on a Büchner funnel with filter paper, washed with EtOH, and stored at –20 °C until further analysis. For comparison, samples treated with either only 8 % MA, only 5 % SHP, or only deionized water were prepared in the same manner (Peng, Yang, & Wang, 2012).

### 2.3.7. Preparation of cellulose treated with compound 1

Whatman filter paper No. 1 (approximately 100 mg) was dipped into an aqueous solution (A or B) containing the cross-linking agent and padded dry using standard laboratory pulp. **Solution A:** 12 % (w/w) compound 1 (as the pentasodium salt, 29 mmol/100 g, 1.0 equiv.) adjusted with H<sub>2</sub>SO<sub>4</sub> (6 M) to pH = 2.0; **solution B:** 12 % (w/w) compound 1 (as the pentasodium salt, 29 mmol/100 g, 1.0 equiv.) and 5 % (w/w) SHP (57 mmol/100 g, 2.0 equiv.) adjusted with H<sub>2</sub>SO<sub>4</sub> (6 M) to pH = 2.0. The procedure was repeated once, reaching a weight gain of approximately 100 %. The sample was dried at 85 °C for 5 min in a laboratory drying oven and cured at 150 °C (alternatively 180 °C) for 5 min in an ashing furnace. Subsequently, the sample was washed with deionized water (approximately 1 L), disintegrated in a kitchen mixer, filtered on a Büchner funnel with filter paper, washed with EtOH, and subsequently stored at –20 °C until further analysis.

### 2.3.8. Treatment of cross-linked fiber samples for FTIR analysis

Approximately 5 mg of pulp sample was suspended in 2 mL of aqueous 0.1 M NaOH in a 4 mL vial and shaken at RT for 5 min. The samples were filtered, washed with an excess of water, and lyophilized for a minimum of 48 h prior to the measurement (Mao & Yang, 2001a).

### 2.3.9. Treatment of cross-linked fiber samples for GPC analysis

Approximately 20 mg of air-dried pulp sample were suspended in 3.0 mL of 0.1 M NaOH in a 4 mL vial and heated to 80 °C in the closed vial using an oil bath for 14 h. The samples were cooled to RT, filtered, washed with an excess of water, briefly washed with 0.05 M HCl, water, and EtOH, and directly prepared for GPC measurements by activation in DMAc and dissolution in DMAc/LiCl 9 % (w/v) (see above).

### 3. Results and discussion

#### 3.1. Mechanistic investigations

In literature, the altered properties of MA/SHP treated fibers are usually attributed to the formation of intermolecular cross-links between cellulose chains (Peng, Yang, & Wang, 2012; Yang et al., 2010). A mechanism has been proposed that involves anhydride formation and subsequent esterification followed by hydrophosphinylation of two MA-cellulose ester moieties with one single SHP molecule (Fig. 1). However, some general chemical and sterical considerations raised questions concerning this pathway and its selectivity. Curing temperatures of 160 °C and higher are likely to cause various transformations and side processes of such reactive substrates, especially with hydrophosphinylations typically proceeding *via* a radical pathway (Montchamp, 2014). Furthermore, the multiple steps of the cross-linking sequence require spatial proximity of all reactants involved in the solid state. Both aspects cast some doubts about the plausibility and especially selectivity of this proposed mechanism. So far, only limited studies to elucidate the reactivity of MA/SHP towards cellulose have been conducted owing to the inherent analytical challenges. With this study, we would like to resume the attempts to address the underlying cross-linking mechanism.

At first, the sequential mechanistic steps were studied individually. Initial activation of MA by dehydration to form its cyclic, intramolecular anhydride, MAH, was reported to be essential for esterification (Yang, 1993). Thus, the minimum temperature for anhydride formation was determined by heating MA to a defined temperature. By  $^1\text{H}$  NMR spectroscopic analysis, the formation of MAH was observed starting from 110 °C, as water is efficiently removed by evaporation at this temperature, and thus the equilibrium is driven towards the product side (see Table S1, SI). As a side reaction, MA isomerized to its thermodynamically more stable *trans*-isomer, fumaric acid (*(E)*-butenedioic acid). After 1 h at 120 °C, only fumaric acid was observed in the  $^1\text{H}$  NMR spectrum, since MAH sublimates at temperatures above 100 °C (Yang et al., 2010). In the cellulose system, it is plausible that highly reactive MAH, once formed by dehydration, almost immediately esterifies spatially close hydroxy groups within a network of cellulosic fibers before undergoing sublimation or isomerization, even at elevated temperatures.

Studies on the temperature-dependence of the esterification of MA and MAH were conducted using 1-octanol as a model compound (see SI, Table S2). After 1 h reaction time at 100 °C, 94.4 % of MAH were converted into the corresponding ester, while only 51.6 % yield (NMR) was achieved in the case of MA. Without an additional catalyst, this

indicates that the esterification proceeds *via* the activated anhydride, as suggested in the literature (Peng, Yang, & Wang, 2012; Yang, 1993). The esterification step was further investigated using MCC (Avicel® PH-101) and MA or MAH at different temperatures. The cellulosic substrate was suspended in an acetone solution of MA or MAH, dried at 75 °C for 15 min, and cured at different temperatures for 30 min. Using a solution-state NMR method for cellulose characterization with  $[\text{P}_{4444}][\text{OAc}]$ :  $\text{DMSO-}d_6$  1:4 (w/w) as the NMR solvent (Fliri et al., 2023; King et al., 2018), the esterified cellulosic moieties were quantified by peak deconvolution of the corresponding quantitative  $^1\text{H}$  NMR spectral areas (see SI, section 2.2 for detailed description). Esterification was confirmed by two coupled doublets at 6.19 and 5.50 ppm, respectively, corresponding to the vicinal CH protons of the MA-ester double bond with a coupling constant of  $J = 11.1$  Hz characteristic of *cis*-alkenes. Covalent esterification of the cellulosic backbone with MA was confirmed by diffusion-edited  $^1\text{H}$  NMR experiments, which filter out the signals from all low-molecular-weight molecules. In agreement with literature reports (Hameed et al., 2016) and observations during the model study, esterification occurred at lower temperatures (starting at 50 °C) when MAH was applied instead of MA, while only minor conversion was observed for MA at 75 °C (see Fig. 2). Quantification of the ester substituents by  $^1\text{H}$  NMR further indicated that saturation occurred at a bulk DS of approximately 0.060 to 0.075. Prolonged reaction time after addition of 1.0 equiv. of MAH did not further increase the MA-cellulose ester signal (Table S3). The rather low DS value, which is a bulk parameter, is explained by the utilization of MCC as a starting material, which is known to exhibit relatively low specific surface area compared to fiber samples. Only the OH groups located on the surface are accessible to esterification, and only a part of them will react as the reaction is rather C6-OH selective (*vide infra*) (Ardizzone et al., 1999; Beaumont et al., 2021). Due to the severe overlap of the residual water signal with the MA functionalities, a rather aggressive baseline correction to remove the water signal was applied to allow at least approximate fitting and integration of the overlapping signals, which of course introduces some additional error. The calculated DS values should thus be considered an estimation rather than a quantitative value (see SI, section 2.2).

In the  $^1\text{H}$ – $^{13}\text{C}$  HSQC spectra of modified MCC, no clear cross peak corresponding to a C6-maleate was apparent due to the overall low DS and associated signal-to-noise issues. In both the diffusion-edited  $^1\text{H}$  and HSQC spectra only two signals for alkene moieties were apparent up to a treatment temperature of 100 °C, before smaller peaks of unsaturated structures appeared at higher temperatures, presumably corresponding to C2/C3-substituted products or *cis/trans*-isomers. It is thus postulated

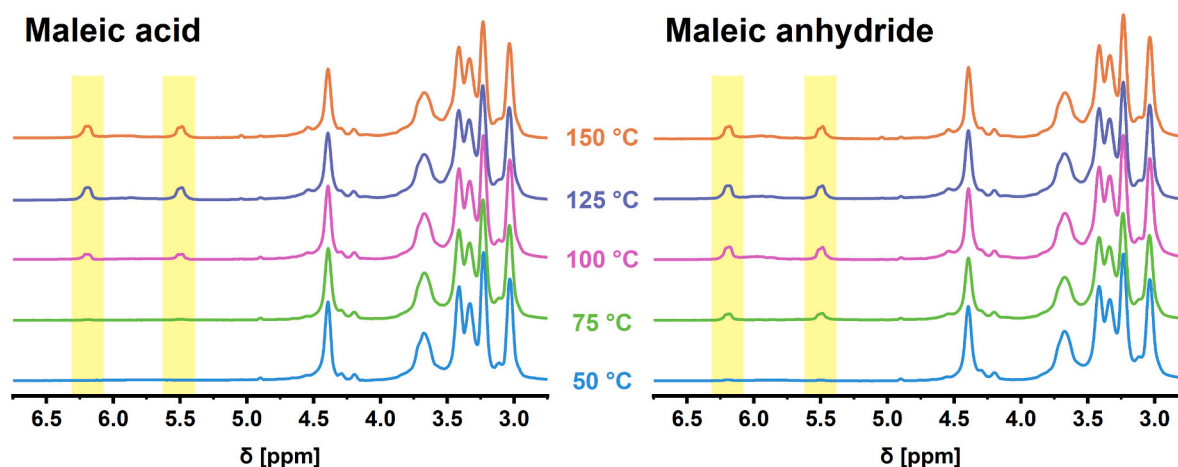


Fig. 2. Solution-state diffusion-edited  $^1\text{H}$  NMR spectra of MCC esterified at different temperatures using MA (left) or MAH (right). The signals of the MA substituents covalently attached to cellulose (at around 5.5 and 6.2 ppm) are highlighted in yellow; signals in the region 2.8 to 5.1 ppm correspond to the cellulosic backbone; signals of low-molecular compounds (such as MA or MAH) are filtered out by the pulse sequence (diffusion-editing).

that such modifications also occur to a low degree, but preferably at the more reactive C6-OH moieties. To further confirm this hypothesis, we used methyl  $\beta$ -D-glucopyranoside as a model compound. As anticipated, esterification predominantly occurred at the C6-OH: a new CH<sub>2</sub> signal corresponding to the 6-position of the MA ester appeared in the <sup>1</sup>H–<sup>13</sup>C HSQC spectrum, while the other CH resonances of the glucopyranose ring remained mostly unchanged. The correlation of this CH<sub>2</sub> to the ester carboxyl (<sup>1</sup>H–<sup>13</sup>C HMBC spectrum) confirmed the covalent bond (see Fig. S1, SI).

### 3.2. Reactivity of sodium hypophosphite

SHP has frequently been stated to act as a catalyst for both anhydride formation and subsequent cellulose esterification (Yang et al., 2010). However, neither a precise catalytic role nor a defined mechanism has been established for the reagent and its reaction with MA. Ji and co-workers studied the SHP/BTCA system stating that anhydride formation might be catalyzed by alkaline metal ions such as K<sup>+</sup>, Na<sup>+</sup>, or Li<sup>+</sup> (added as the corresponding hydroxide directly into the dipping solution) by decreasing the H-bond interactions between the carboxyl groups of BTCA (Ji et al., 2016). However, no study confirming this hypothesis by the addition of a neutral salt, e.g., NaCl, was conducted. Thus, this effect might also be caused by a difference in pH due to the higher basicity of the alkali hydroxides compared to SHP. For an aromatic polycarboxylic acid – 3,3',4,4'-benzophenone tetracarboxylic acid (BPTCA) – Zhao and Sun reported cellulose esterification following an acid-catalyzed Fischer mechanism rather than a two-step mechanism via the corresponding anhydride. As catalysts, sodium salts of different acids exhibiting a low pKa and little steric hindrance of the anion, such as SHP, monosodium phosphate, and sodium dichloroacetate, were used and an optimum pH of 1.8–2.0 was stated (Hou & Sun, 2013; Zhao & Sun, 2015).

To investigate the role of SHP during anhydride formation, MA and an equimolar amount of SHP were heated as a powdered mixture. The solid-state reaction between these reagents was previously examined by Yang and co-workers using FTIR spectroscopy and thermal gravimetric analysis (TGA), but no detailed analyses regarding the chemical structure of the products have been conducted (Yang et al., 2010), although FTIR bands associated with the HC=CH bond at 3060 cm<sup>-1</sup> decreased in intensity. To identify the phosphorus-containing products, we used <sup>31</sup>P NMR in both <sup>1</sup>H-decoupled and non-decoupled modes. Additionally, <sup>1</sup>H–<sup>31</sup>P HMBC experiments were performed to identify short-range and long-range <sup>1</sup>H–<sup>31</sup>P couplings. Owing to the wide range of chemical shifts in <sup>31</sup>P NMR spectroscopy (>500 ppm), even minor changes in the binding situation and resulting differences in electronic shielding of the phosphorus atom often induce considerable chemical shift differences (Gorenstein & Luxon, 1999). Consequently, the chemical shift is also highly affected by the pH and concentration of the sample solution. Therefore, referencing of the shifts is challenging and <sup>31</sup>P NMR spectra were rather used as a qualitative measure and for determination of the H–P couplings.

Solution-state NMR spectroscopy revealed the formation of different products at temperatures above 80 °C, with only minimal amounts of MAH being formed, contrasting pure MA conditions (Fig. 3; for details see Table S3, SI). Salt metathesis of MA and SHP resulted in an equilibrium with monosodium maleate and phosphinic acid, the conjugated acid to SHP, due to their quite similar pKa values (pKa1 (MA) = 1.92 (Hussain et al., 2003); pKa (H<sub>3</sub>PO<sub>2</sub>) = 1.24 (Greenwood & Earnshaw, 1997)). The formation of phosphinic acid was confirmed by an increase of the <sup>1</sup>J<sub>P,H</sub> coupling constant from 452 to 490 Hz while retaining the triplet resonance in the non-decoupled <sup>31</sup>P NMR spectrum, which is characteristic of the H–P–H moiety. Protonation of SHP with one equivalent of HCl in a control experiment also resulted in an increase in the coupling constant to 540 Hz, which is in agreement with the literature (Moedritzer, 1967). Further, the mono-hydrophosphinylated product, formed by the addition of SHP to the MA double bond, was

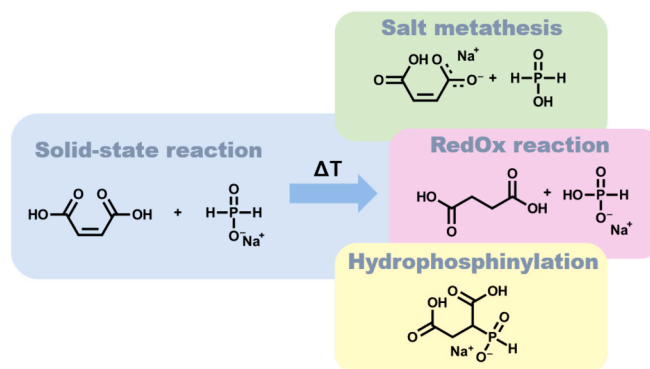


Fig. 3. Summary of the reactivity of MA and SHP at elevated temperature. Reagents were mixed in the solid state and heated to different temperatures; the displayed products were identified from the NMR spectra of the product mixtures.

observed. In the <sup>1</sup>H–<sup>31</sup>P HMBC spectrum, the compound showed cross-peaks of the phosphorus atoms ( $\delta_P = 21.30$  and 19.68 ppm) in the P–H moiety at  $\delta_H = 6.94$  ppm (d,  $J = 518$  Hz) with the CH-protons at  $\delta_H/\delta_C = 2.74/45.42$  ppm and the CH<sub>2</sub>-protons at  $\delta_H/\delta_C = 2.55/30.26$  ppm. Moreover, succinic acid and an oxidized phosphorus species with one H directly bound to P were observed, when extending reaction times or curing at higher temperatures. The corresponding doublet at 6.66 ppm in the <sup>1</sup>H NMR spectrum (<sup>1</sup>J<sub>P,H</sub> = 616 Hz) was attributed to an equilibrium mixture of H<sub>3</sub>PO<sub>3</sub> and sodium phosphinate. Hypophosphite is known as a potent reducing agent, resulting in the formation of phosphite and transient atomic H in redox reactions involving H<sub>2</sub>O (Guyon et al., 2015; Liu et al., 2017). The nascent H is highly reactive and thus prone to reduce unsaturated hydrocarbons, as in the case of MA. The succinic acid formed thereby exhibits a much higher activation energy for intramolecular anhydride formation than MA. This redox reaction additionally lowers the yield of any potential cross-linking products. Consequently, esterification of cellulose via the proposed anhydride would require a higher temperature and P-bridged cross-links cannot be formed due to the lack of a C=C bond necessary for hydrophosphinylation to proceed.

Investigating the catalytic effect of SHP during the esterification of cellulose with BTCA, Ji and co-workers suspected that SHP enhances the deprotonation of the hydroxy group as an alkaline catalyst (Ji et al., 2015). However, if and how this anionization would promote ester formation is rather unclear. Our findings indicate that in the MA/SHP system, SHP is protonated by MA under such acidic conditions rendering an alkaline catalysis rather unlikely, thus contradicting the catalytic role attributed to SHP in the anhydride formation and esterification. It can be safely stated that these reaction steps do not proceed selectively and do not form the corresponding ester in any significant yields in the model reactions. Instead, we observed multiple reaction paths of SHP/MA, i.e., metathesis, reduction/oxidation, and hydrophosphinylation, proceeding already at short curing times.

### 3.3. Cross-link formation

The formation of covalent, phosphorus-bridged cross-links has been reported to occur at significantly elevated temperatures through the reaction of SHP with the olefinic bond of the previously formed MA-ester (Peng, Yang, & Wang, 2012; Yang et al., 2010). Hydrophosphinylation, the addition of phosphinate to unsaturated hydrocarbons, can generally occur either in a (transition)metal-catalyzed reaction or according to a radical pathway (Montchamp, 2014). In the absence of a radical initiator or catalyst, the homolytic (radical) pathway requires high temperatures to overcome the P–H bonding energy for homolytic cleavage before radical addition can occur. For SHP, which possesses a geminal PH<sub>2</sub> moiety, the reaction of the first P–H occurs rather readily, while higher

energy is required for the release of the second hydrogen because the bond dissociation energy of the P—H bond in hypophosphites is generally lower than in case of *H*-phosphinates (in which one H of the hypophosphite is already replaced by an alkyl moiety). This is because in phosphinates (with at least one direct P—H bond) the phosphinylidene moiety P(O)-H can tautomerize to form P-OH, which decreases P—H reactivity. In the case of mono-alkylated *H*-phosphinates with electron-withdrawing groups (EWGs) as substituents, such as the succinyl moiety, the OH-form is even more favored due to the stabilizing effect of the EWG on the P's free lone electron pair, which renders the P—H less reactive (Montchamp, 2014). Consequently, di-substitutions of hypophosphites, *i.e.* bis-additions to two olefinic moieties, require high temperatures or a large excess of the alkene component (Markoulides & Regan, 2012).

Model reactions assessing the reactivity of MA, SHP, and an alcohol moiety (for ester formation) were performed and analyzed by NMR spectroscopy. Cyclohexanol, 1-octanol, or 1-hexanol were selected as alcohol components for analytical reasons (good separation and spectral clarity). The reagents were mixed and heated to >130 °C to simulate the curing process/cross-linking treatment. Besides the reaction products of MA and SHP already observed at lower temperatures, both mono- and di-addition products were also identified in the resulting mixture, due to a characteristic coupling in the <sup>31</sup>P NMR spectra. The di-alkylphosphinate results in a singlet in both the <sup>1</sup>H-decoupled and the non-decoupled <sup>31</sup>P spectrum, because no H is directly bonded to the phosphorus, while the mono-alkylated *H*-phosphinate gives a doublet in the non-decoupled spectrum. Additionally, <sup>31</sup>P NMR resonances of phosphinates are downfield shifted with increasing alkyl substitution and substituent bulkiness due to the deshielding —I effect of the substituents on the phosphorus atom (Kühl, 2008). However, no individual neat product was isolated from the complex mixtures. Variation of molar ratios did not increase the selectivity of the reaction significantly (see also Parsons & Wright, 2008). Further, differences between using a one-pot and a stepwise approach (preliminary esterification of MA with 1-octanol and subsequent hydrophosphinylation attempt with SHP) were negligible. Representative NMR spectra of the respective product mixtures are provided in the SI (Figs. S2 and S3). Essentially all <sup>31</sup>P spectra showed multiple signals confirming a mixture of numerous different phosphorus-containing products besides the target di-alkyl phosphinate. Our findings clearly demonstrate that a neat cross-link formation does not occur. The selectivity in the model compound reaction was rather low, and even though some of the desired bis-addition product was observed, it was accompanied by a plethora of byproducts. We thus assume a similar reactivity and even lower selectivity for the cellulose case, in which steric and accessibility reasons disfavor dialkyl phosphinate formation with the celluloses' hydroxyl groups compared to the easily accessible model alcohols.

### 3.4. Treatment of cellulose

Cellulose was treated with MA and SHP according to a literature procedure implementing minor modifications based on equipment availability (Peng, Yang, & Wang, 2012). Whatman paper No. 1 was chosen as a well-characterized cellulosic substrate exhibiting good solubility for ready GPC analysis. For FTIR spectroscopic analysis, free C(O) OH (carboxyl) groups were converted into the respective sodium salts (carboxylate) by NaOH treatment (0.1 M NaOH, RT, 5 min) to eliminate overlapping of the ester and acid carbonyl band (Mao & Yang, 2001b). The corresponding spectra indicate the formation of ester bonds at 1719 cm<sup>-1</sup> (see SI, Fig. S13). Due to the insolubility of the cellulosic product in the electrolyte [P<sub>4444</sub>][OAc]:DMSO-*d*<sub>6</sub> (1:4 w/w), the covalent linkage of the treated samples could not be confirmed directly by solution-state NMR. Solid-state CP/MAS <sup>13</sup>C NMR measurements showed a broad signal in the C=O region at 173.5 ppm. However – in contrast to literature statements (Hameed et al., 2016) – the observation of signals in the carboxyl region cannot be seen as a definite proof for covalent cross-

linking. Without 2D NMR experiments, C(O)OH and C(O)OR functionalities cannot be clearly distinguished. Moreover, the presence of any ester signals confirms only the esterification of cellulose, but not the formation of cross-links following the suggested phosphorus-bridging mechanism, as esterification takes place at a lower temperature than the hydrophosphinylation (see above).

The influence of the cross-linking treatment on the molecular weight distribution of cellulose was investigated by GPC-MALLS in the eluent DMAc/LiCl 0.9 % (w/v) (Potthast et al., 2015). Direct molecular weight determination of cross-linked fiber samples using this solvent system was not possible due to the insolubility of the samples. This was also true for MA-only treated samples and samples treated with lower concentrations of cross-linking agents, while SHP-only treated samples and blanks were still well soluble after curing. Thus, we cleaved the cross-links by NaOH treatment (0.1 M NaOH, 80 °C, 14 h), targeting hydrolysis of the ester linkages to enable analytical characterization. In this way, the influence of the cross-linking treatment on the molecular weight of the fiber substrate was studied. Subsequent GPC analysis showed a significant reduction of molecular weight after MA/SHP treatment from M<sub>w</sub> = 268.7 to 171.7 kg/mol (Table 1, entry B5 and S1; Fig. 4 A). Some degradation might be attributed to the oxidation of the cellulose during heat treatment (M<sub>w</sub> = 284.3 to 269.4 kg/mol, entry B2 and B5), followed by beta-elimination reactions in the alkaline medium (Hosoya et al., 2018) used for ester hydrolysis. However, acidic hydrolysis might also significantly contribute to chain cleavage, as the treatment solution in the case of S1 is strongly acidic (pH = 1.65) (Emsley et al., 1997; Mozdyniewicz et al., 2016). The involvement of radical species in cellulose degradation can neither be proven nor disproven based on the available experimental data. On the one hand, since SHP is prone to form radicals at high temperatures and was proven to undergo radical reactions, especially with a suitable co-reactant present, such as MA, the formation of free radical species is likely to account for some of the degradation effects. However, on the other hand, SHP is also considered to be an antioxidant, so its homolytic reactions might be self-inhibiting, as phosphorus-based antioxidants were described to significantly mitigate autoxidation by hydroperoxides (Jeong et al., 2014). Upon reduction of the curing temperature from 180 to 150 °C, degradation after NaOH treatment was limited in blank samples (entry B1 vs. B2 without NaOH treatment). These results indicate enhanced cellulose oxidation at higher temperatures forming C=O moieties in the cellulose backbone. Under alkaline conditions, these oxidized groups, representing oxidative “hot spots”, cause chain cleavage by β-alkoxy-elimination (see above). Thus, a reduction of the curing temperature is beneficial to maintain cellulose integrity and the lifetime of the fibers.

### 3.5. A related, alternative cross-linking approach

Condensation of MA and SHP under defined conditions prior to application onto the cellulosic material was used as an alternative, improved cross-linking approach, mainly for two reasons: Firstly, pre-condensation enables defined cross-links in a better controlled and more atom-efficient way. As our mechanistic studies revealed, phosphorus-bridged cross-links are not at all formed selectively, and multiple side products were observed under conditions of the standard cross-linking procedure reported in the literature. This means that only a small amount of the reagents used actually contributes to cross-linking. Secondly, pre-condensation might enable efficient cross-linking already under much milder conditions. By avoiding the high temperatures necessary for radical hydrophosphinylation of *H*-phosphinates on the cellulosic substrate, degradation of the latter can be significantly limited, as blank studies indicated (see Table 1, entry B1-B5).

The cross-linker sodium 2-[(1,2-dicarboxylethyl)phosphinate]succinic acid (compound 1) was synthesized by hydrophosphinylation of MA in an alkaline aqueous medium using Na<sub>2</sub>S<sub>2</sub>O<sub>8</sub> as a radical initiator (Fig. 5). The synthesis was conducted similarly to published protocols (Gardner et al., 2006; Sivik et al., 2007), with some minor modifications

**Table 1**

GPC analysis of treated fiber samples. All samples were dipped into the specific curing solution (MA/SHP, compound 1, compound 1/SHP for samples S1-S5 or water for blanks B1-B5), dried at 85 °C for 5 min and then cured for 5 min at the specified temperature unless indicated otherwise. NaOH treatment (0.1 M NaOH, 80 °C, 14 h) was conducted to open ester cross-links and thus enable dissolution in DMAc/LiCl 9 % (w/v) for GPC analysis.

| Entry     | Treatment      | Curing T [°C] | NaOH treatment | M <sub>n</sub> [kg/mol] | M <sub>w</sub> [kg/mol] | M <sub>z</sub> [kg/mol] | D   |
|-----------|----------------|---------------|----------------|-------------------------|-------------------------|-------------------------|-----|
| Reference | –              | –             | –              | 172.3                   | 368.2                   | 617.3                   | 2.1 |
| B1        | –              | 150           | –              | 130.7                   | 280.6                   | 503.9                   | 2.2 |
| B2        | –              | 180           | –              | 118.6                   | 284.3                   | 545.7                   | 2.4 |
| B3        | –              | –             | +              | 136.7                   | 269.8                   | 441.1                   | 2.0 |
| B4        | –              | 150           | +              | 118.4                   | 236.8                   | 401.7                   | 2.0 |
| B5        | –              | 180           | +              | 125.1                   | 268.7                   | 445.9                   | 2.2 |
| S1        | MA/SHP         | 180           | +              | 55.9                    | 171.7                   | 408.5                   | 3.1 |
| S2        | Compound 1     | 150           | +              | 48.5                    | 163.3                   | 394.6                   | 3.4 |
| S3        | Compound 1/SHP | 150           | +              | 87.0                    | 235.1                   | 509.4                   | 2.7 |
| S4        | Compound 1     | 180           | +              | 34.5                    | 126.5                   | 311.7                   | 3.7 |
| S5        | Compound 1/SHP | 180           | +              | 74.5                    | 244.1                   | 593.3                   | 3.3 |

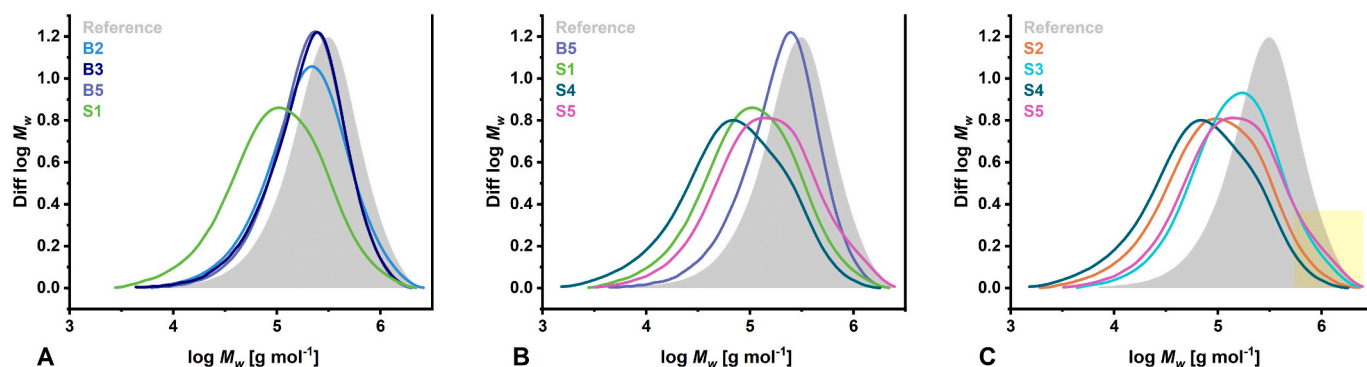


**Fig. 4.** Normalized molecular weight distributions of treated fiber samples after cleavage of the ester-linkages by NaOH treatment; MWD of the starting material shown in grey (Reference); A: cellulose degradation of blank samples caused by curing at 180 °C (B2), NaOH treatment (B3) and both (B5) compared to MA/SHP cross-linking treated sample (S1); B: MWD of literature treated sample (S1) compared to samples treated with 1 (S4) and 1/SHP (S5) at 180 °C; C: curing temperature-dependent degradation of 1-treated samples cured at 150 °C (S2, S3) and 180 °C (S2, S3), residual high MW fractions highlighted in yellow. Conditions for all samples are specified in Table 1.

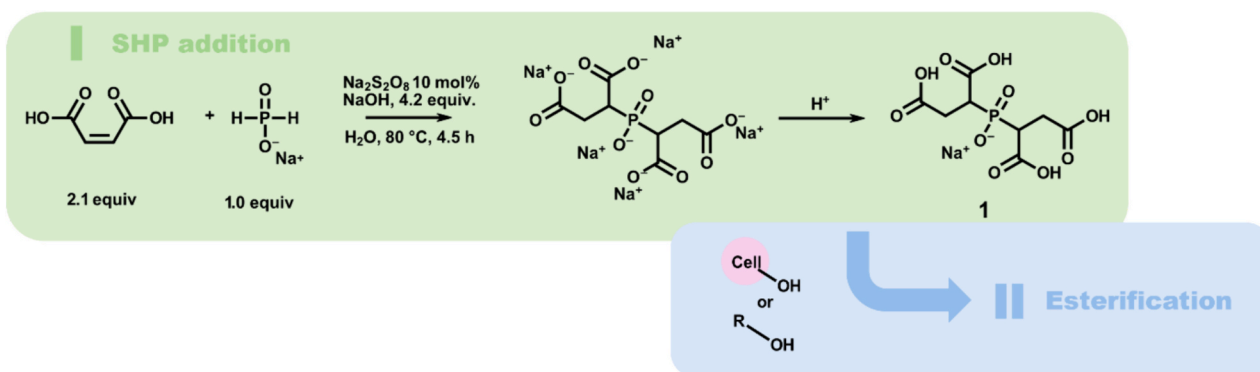


**Fig. 5.** Synthesis of cross-linker 1 by pre-condensation of MA and SHP by radical hydrophosphinylation and subsequent esterification of cellulosic OH groups.

targeting the isolation of a pure compound with a well-defined structure which would allow for better control of the cross-linking process. In previous protocols, mainly mixtures of PMA were obtained by partial deprotonation of MA prior to condensation, and the reaction mixture was directly used after synthesis without further purification or isolation of the components (Chen et al., 2005; Cheng & Yang, 2009). In a recent publication about the addition of hypophosphite to alkenes, Huang and co-workers reported that full maleate deprotonation and a certain ratio of SHP to MA were crucial for obtaining high yields of the *H*-phosphinate (Huang et al., 2022). We found similar requirements to be also true for the synthesis of the di-alkylated product. While under acidic conditions a mixture of higher molecular weight P–H adducts is yielded due to

competing polymerization (Chen et al., 2005), the desired product was obtained rather selectively in an alkaline medium. The higher electron density at the C=C bond after deprotonation of MA seems to inhibit the polymerization reaction, which might be attributed to insufficient charge stabilization due to limited mesomeric structures. Upon acidification, the protonated species was obtained and characterized by NMR and LC-MS. In all NMR spectra, double the number of signals expected from the anticipated structure of compound 1 was observed (see SI, Figs. S4 and S5). Reversed-phase LC-ESI-MS measurements revealed a double peak with two maxima at retention times of 2.019 and 2.118 min, both with the same *m/z* value of 299.016 corresponding to the molecular weight of the fully protonated structure of 1 (Fig. 6). This is

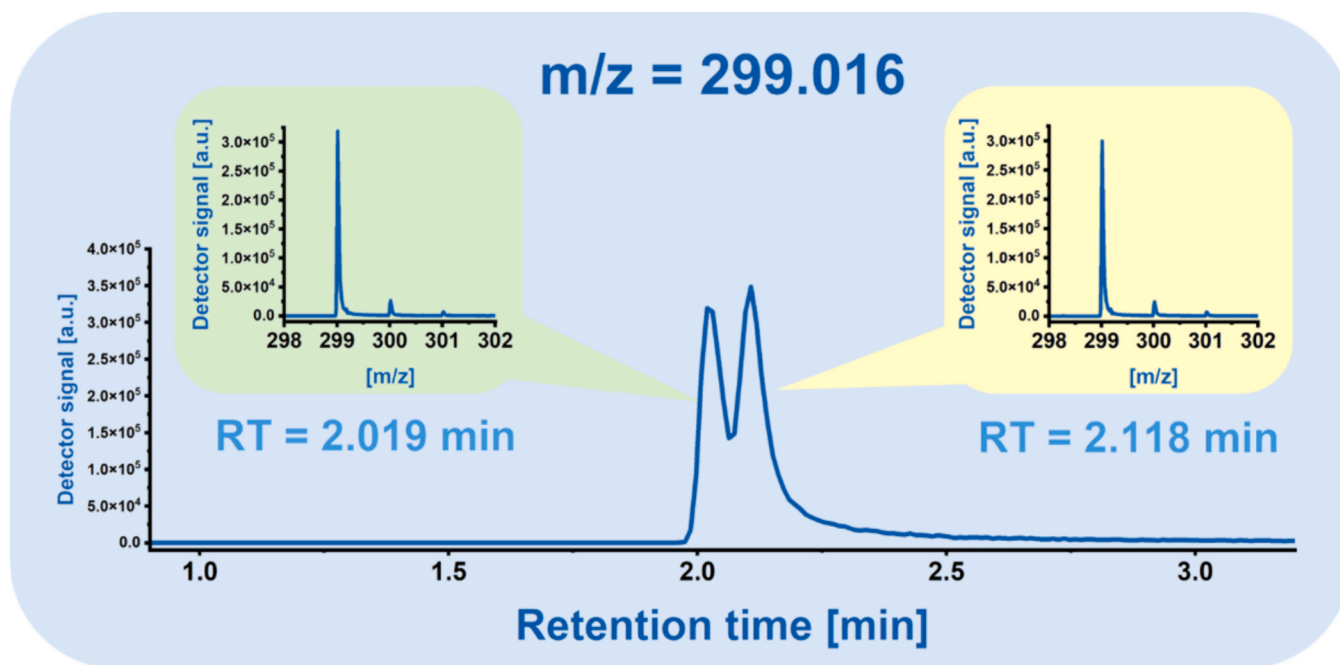


Fig. 6. LC-ESI-MS chromatogram of compound **1**. ESI-MS spectra of the respective peaks were obtained in scan mode. At RT = 2.019 min and 2.118 min, the main  $m/z$  found was 299.016 corresponding to the fully protonated species of **1** [ $M + H^+$ ].

due to the fact that compound **1** exhibits two chiral carbons directly bound to the phosphorus. Thus, four stereoisomers result from each combination of (*R*) and (*S*) configuration (see SI, Fig. S11). Although NMR spectroscopy and liquid chromatography cannot fully separate all of them, the major structural difference between the two identical, achiral *meso*-structures (*RS* and *SR*) and the other chiral stereoisomers (*SS* and *RR* enantiomers) can indeed be detected, resulting in a 1:1 intensity ratio of the resulting signals. By further separation of the two enantiomers, we hypothesize a 2:1:1 ratio corresponding to the *meso*:*SS*:*RR* compounds. Attempts to further separate the stereoisomers of **1** by chiral anion-exchange HPLC are ongoing work.

NMR spectra of **1** recorded at different pH values of the sample solution resulted in shifted signals, however, the exact pKa values of the compound have not been determined so far. Chen and co-workers stated that titration curves of saturated polycarboxylic acids such as BTCA and SA typically do not give defined pKa values but rather show a gradual increase in pH upon base addition (Chen et al., 2005). It is anticipated that the pKa values of the carboxyl groups in compound **1** are in the range of succinic acid (pKa1 = 4.21; pKa2 = 5.64), while the pKa of the di-alkyl phosphinic acid is highly dependent on the alkyl substituents, ranging from pKa = 3.1 down to 1.0 (Dhaene et al., 2022; Viveros-Ceballos et al., 2016; Wang et al., 2017). Thus, it can be expected that at pH = 1–2, a sufficient number of carboxylates is protonated and therefore ready to undergo esterification.

### 3.6. Reactivity of compound **1** in esterification reactions

The reactivity of **1** in an uncatalyzed esterification reaction was tested using 1-hexanol as a model alcohol, by heating the mixture to 120 °C. The formation of the corresponding ester was confirmed by NMR spectroscopy. Hence, compound **1** was applied to cellulose analogously to the MA/SHP cross-linking method. A 0.3 M aqueous solution of **1** was prepared and the pH was adjusted to 2 with H<sub>2</sub>SO<sub>4</sub> (4 M) to protonate the cross-linker. For comparison, a second solution containing 0.3 M **1** and 0.3 M SHP was prepared at pH 2. Whatman paper samples were dipped, dried, and cured at 150 and 180 °C before washing. The dried samples showed bands indicative of ester formation in the FTIR and <sup>13</sup>C solid-state NMR spectra almost identical to the MA/SHP treated

samples. As in the case of the latter (see above), samples treated with compound **1** were insoluble and thus not suitable for solution-state NMR spectroscopy or GPC-MALLS analysis. Thus, the samples were subjected to cleavage of the ester bonds by NaOH treatment prior to GPC analysis. In accordance with the MA/SHP treatment, all samples showed a significant reduction in M<sub>w</sub> (Table 1, entries S2–S5). In contrast to our initial assumption of highly reactive SHP-centered radicals contributing to chain cleavage, we found that the degradation was significantly limited when compound **1** was combined with SHP in an equimolar ratio compared to treatment with pure compound **1**. Although not yet experimentally confirmed, this phenomenon is likely to be a result of SHP acting as an antioxidant during curing. Further, compound **1**/SHP-treated samples show a shoulder in the high molecular weight range of the MWD curves, indicating that some of the formed cross-links survived NaOH hydrolysis (Fig. 4, B3 and B5, highlighted in yellow). Thus, **1** in combination with an equimolar amount of SHP might be a highly effective cross-linker, superior to the conventionally used alternatives, which additionally contributes to the protection of cellulose fibers during high-temperature curing. The definite proof of covalent cross-links by the system **1**/SHP and the confirmation of the role of SHP as an antioxidant and stabilizer of cellulose integrity are topics of work currently ongoing.

## 4. Conclusions and outlook

Mechanistic investigations on cross-linking with MA and SHP were conducted by targeting the sequential steps of the mechanism suggested in the literature individually, *i.e.*, MA esterification, SHP addition, and cross-link formation. We aimed to resume the attempts to address the underlying cross-linking mechanism, using both model compounds and cellulosic substrates and implementing a combination of appropriate analytical techniques to better address the mode of action of the MA/SHP treatment. We found that esterification took place at a lower temperature when using MAH instead of MA, thereby supporting the literature hypothesis of anhydride formation proceeding as the initial reaction step. However, upon the addition of SHP to MA moieties, multiple side reactions at elevated temperatures were observed leading to the formation of product mixtures rather than a defined reaction

product. These might prevent cross-linking according to the reported mechanism, most notably by the reduction of maleate to succinate compounds by SHP. For effective and selective cross-link formation, two esterified MA-cellulose moieties must be in sufficient spatial proximity and appropriate geometry to react one after the other with one single hypophosphite molecule, which is difficult to achieve in this solid-state reaction. Due to these factors, MA/SHP cross-linking efficiency and yield are hard to control, challenging to determine, and not selectively proceeding according to the pathway reported in the literature. Consequently, the altered properties of treated fabrics, such as wrinkle or fibrillation resistance, might only be partially caused by actual covalent cross-link formation, as proposed in the literature (Ji et al., 2016). Other chemical reactions between cellulose and the finishing reagents, such as a change in hydrophobicity, or simple physical phenomena can cause the observed effect.

Targeting more selective cross-linking, we synthesized a well-defined cross-linker, 2-[(1,2-dicarboxyethyl)phosphinate]succinic acid (**1**) in a rather mild hydrophosphinylation reaction similar to patent literature procedures, characterized it comprehensively, and conducted preliminary tests regarding its reactivity in esterification. In a reaction with a model compound, we observed ester formation in NMR spectroscopy and thus assumed that this was also true for cellulosic substrates. Owing to the insolubility of the treated samples in DMAc/LiCl 9 % (w/v) – a sign of cross-linking having occurred – the MWs were determined by GPC-MALLS after alkaline treatment to remove covalent cross-links. While conventional (literature) treatment with MA/SHP led to significant degradation of cellulose chains, compound **1**/SHP treatment retained higher molecular masses. Our results indicate that this might be attributed to the reductive/antioxidant nature of SHP as an additive during curing. Further experimental evidence is necessary to unambiguously prove this hypothesis. Studies regarding the optimization of treatment conditions and fabric properties on the cross-linking system of compound **1**/SHP are ongoing.

#### Declaration of competing interest

The authors declare that they have no known competing financial interests or personal relationships that could have appeared to influence the work reported in this paper.

#### Data availability

Data will be made available on request.

#### Acknowledgments

The authors are grateful to the University of Natural Resources and Life Sciences, Vienna (BOKU), the BOKU doctoral school “Advanced Biorefineries: Chemistry & Materials” (ABC&M), and the County of Lower Austria through the framework of the Austrian Biorefinery Center Tulln (ABCT-II) for their financial support. The financial support by the GFF Gesellschaft für Forschungsförderung Niederösterreich m.b.H. (A.F. L. and H.H., project LSC20-002) is gratefully acknowledged. Analytical equipment was kindly provided by the BOKU Core Facility ALICE. We thank Daniel Maresch, BSc., for conducting MS experiments. The MS equipment was kindly provided by the EQ-BOKU VIBT GmbH and the BOKU Core Facility Mass Spectrometry.

#### CRediT authorship contribution statement

**AFL:** conceptualization, investigation, visualization, data curation, writing—original draft, writing—review and editing. **LF:** conceptualization, investigation, data curation, writing—review and editing. **MB:** data curation, writing—review and editing. **DB:** data curation, visualization. **IS:** data curation, writing—review and editing. **MH:** supervision, conceptualization, resources, writing—review and editing, project

administration. **TR:** conceptualization, writing—review and editing, supervision, project administration. **HH:** conceptualization, writing—review and editing, supervision, funding acquisition, project administration.

All authors have read and approved the manuscript.

#### Funding

Open Access funding is provided by the University of Natural Resources and Life Sciences, Vienna (BOKU).

#### Ethics approval and consent to participate

Not applicable.

#### Consent for publication

All authors agreed to the publication in the submitted form.

#### Appendix A. Supplementary data

Supplementary data to this article can be found online at <https://doi.org/10.1016/j.carbpol.2024.122653>.

#### References

- Ardizzone, S., Dioguardi, F. S., Mussini, T., et al. (1999). Microcrystalline cellulose powders: Structure, surface features and water sorption capability. *Cellulose*, 6, 57–69. <https://doi.org/10.1023/A:1009204309120>
- Beaumont, M., Tardy, B. L., Reyes, G., Koso, T. V., Schaubmayr, E., ... Jusner, P. Rosenau (2021). Assembling native elementary cellulose nanofibrils via a reversible and regioselective surface functionalization. *Journal of the American Chemical Society*, 143 (41), 17040–17046.
- Chen, D., Yang, C. Q., & Qiu, X. (2005). Aqueous polymerization of maleic acid and cross-linking of cotton cellulose by poly(maleic acid). *Industrial and Engineering Chemistry Research*, 44, 7921–7927. <https://doi.org/10.1021/ie050651+>
- Cheng, X., & Yang, C. Q. (2009). Flame retardant finishing of cotton fleece fabric: Part V. Phosphorus-containing maleic acid oligomers. *Fire and Materials*, 33, 365–375. <https://doi.org/10.1002/fam.1008>
- Davis, C. S., Johnson, M. K., & Richardson, R. J. (1985). Organophosphorus compounds. *Neurotoxicity of industrial and commercial chemicals*, 2.
- Dhaene, E., Pokratath, R., Aalling-Frederiksen, O., et al. (2022). Monoalkyl Phosphinic acids as ligands in nanocrystal synthesis. *ACS Nano*, 16, 7361–7372. <https://doi.org/10.1021/acsnano.1c08966>
- Emsley, A. M., Heywood, R. J., Ali, M., & Eley, C. M. (1997). On the kinetics of degradation of cellulose. *Cellulose*, 4, 1–5. <https://doi.org/10.1023/A:1018408515574>
- Fliri, L., Heise, K., Koso, T., et al. (2023). Solution-state nuclear magnetic resonance spectroscopy of crystalline cellulosic materials using a direct dissolution ionic liquid electrolyte. *Nature Protocols*, 1–45. <https://doi.org/10.1038/s41596-023-00832-9>
- Gardner RR, Scheper WM, Sivik MR, Arredondo VM (2006) Shrink resistant and wrinkle free textiles.
- Gorenstein, D. G., & Luxon, B. A. (1999). 31 P NMR. In: *Encyclopedia of Spectroscopy and Spectrometry*. Elsevier, 2204–2212.
- Granzow, A. (1978). Flame retardation by phosphorus compounds. *Accounts of Chemical Research*, 11, 177–183. <https://doi.org/10.1021/ar50125a001>
- Phosphorus. In Greenwood, N. N., & Earnshaw, A. (Eds.), *Chemistry of the elements (second edition)*. (pp. 473–546). (1997) (pp. 473–546). Oxford: Butterworth-Heinemann.
- Guyon, C., Métay, E., Popowycz, F., & Lemaire, M. (2015). Synthetic applications of hypophosphite derivatives in reduction. *Organic & Biomolecular Chemistry*, 13, 7879–7906. <https://doi.org/10.1039/C5OB01032B>
- Hameed, S., Hussain, M. A., Masood, R., & Haseeb, T. (2016). Cross-linking of cotton fabric using maleic anhydride and sodium hypophosphite. *Cellulose Chem Technol*, 50, 321–328.
- Hosoya, T., Bacher, M., Potthast, A., et al. (2018). Insights into degradation pathways of oxidized anhydroglucose units in cellulose by  $\beta$ -alkoxy-elimination: A combined theoretical and experimental approach. *Cellulose*, 25, 3797–3814. <https://doi.org/10.1007/s10570-018-1835-y>
- Hou, A., & Sun, G. (2013). Multifunctional finishing of cotton fabrics with 3,3',4,4'-benzophenone tetracarboxylic dianhydride: Reaction mechanism. *Carbohydrate Polymers*, 95, 768–772. <https://doi.org/10.1016/j.carbpol.2013.02.027>
- Hu, H., Li, F., Cai, T., et al. (2022). Synthesis of novel poly-carboxylic acids via click reaction and their application for easy-care treatment of cotton fabrics. *Cellulose*, 29, 9437–9452. <https://doi.org/10.1007/s10570-022-04825-x>
- Huang, Z., Chen, Y., & Kanan, M. W. (2022). Hypophosphite addition to alkenes under solvent-free and non-acidic aqueous conditions. *Chemical Communications*, 58, 2180–2183. <https://doi.org/10.1039/D1CC06831H>

- Hussain, S., Pinitglang, S., Bailey, T. S. F., et al. (2003). Variation in the pH-dependent pre-steady-state and steady-state kinetic characteristics of cysteine-proteinase mechanism: Evidence for electrostatic modulation of catalytic-site function by the neighbouring carboxylate anion. *Biochemical Journal*, 372, 735–746. <https://doi.org/10.1042/bj20030177>
- Jeong, M.-J., Dupont, A.-L., & De La Rie, E. R. (2014). Degradation of cellulose at the wet-dry interface. II. Study of oxidation reactions and effect of antioxidants. *Carbohydrate Polymers*, 101, 671–683. <https://doi.org/10.1016/j.carbpol.2013.09.080>
- Ji, B., Qi, H., Yan, K., & Sun, G. (2016). Catalytic actions of alkaline salts in reactions between 1,2,3,4-butanetetracarboxylic acid and cellulose: I. *Anhydride formation*. *Cellulose*, 23, 259–267. <https://doi.org/10.1007/s10570-015-0810-0>
- Ji, B., Tang, P., Yan, K., & Sun, G. (2015). Catalytic actions of alkaline salts in reactions between 1,2,3,4-butanetetracarboxylic acid and cellulose: II. *Esterification*. *Carbohydrate Polymers*, 132, 228–236. <https://doi.org/10.1016/j.carbpol.2015.06.070>
- King, A. W. T., Mäkelä, V., Kedzior, S. A., et al. (2018). Liquid-state NMR analysis of Nanocelluloses. *Biomacromolecules*, 19, 2708–2720. <https://doi.org/10.1021/acs.biomac.8b00295>
- Koso, T., Rico del Cerro, D., Heikkinen, S., et al. (2020). 2D assignment and quantitative analysis of cellulose and oxidized celluloses using solution-state NMR spectroscopy. *Cellulose*, 27, 7929–7953. <https://doi.org/10.1007/s10570-020-03317-0>
- Kühl, O. (2008). *Phosphorus-31 NMR spectroscopy: A concise introduction for the synthetic organic and organometallic chemist*. Berlin Heidelberg: Springer.
- Liang, T., Yan, K., Zhao, T., & Ji, B. (2020). Synthesis of a low-molecular-weight copolymer by maleic acid and acrylic acid and its application for the functional modification of cellulose. *Cellulose*, 27, 5665–5675. <https://doi.org/10.1007/s10570-020-03201-x>
- Liu, D., Li, X., Wei, L., et al. (2017). Disproportionation of hypophosphite and phosphite. *Dalton Transactions*, 46, 6366–6378. <https://doi.org/10.1039/C7DT00243B>
- Liu, J., Wang, B., Xu, X., et al. (2016). Green finishing of cotton fabrics using a xylitol-extended citric acid cross-linking system on a pilot scale. *ACS Sustainable Chemistry & Engineering*, 4, 1131–1138. <https://doi.org/10.1021/acsschemeng.5b01213>
- Liu, J., Wang, H., Zhang, L., et al. (2019). Preparation, structure and performances of cross-linked regenerated cellulose fibers. *Wuhan University*, 24, 1–7. <https://doi.org/10.1007/s11859-019-1361-2>
- Ma, Y., Rissanen, M., You, X., et al. (2021). New method for determining the degree of fibrillation of regenerated cellulose fibres. *Cellulose*, 28, 31–44. <https://doi.org/10.1007/s10570-020-03513-y>
- Ma, Y., You, X., Rissanen, M., et al. (2021). Sustainable cross-linking of man-made cellulosic fibers with poly(carboxylic acids) for fibrillation control. *ACS Sustainable Chemistry & Engineering*, 9, 16749–16756. <https://doi.org/10.1021/acsschemeng.1c06101>
- Mao, Z., & Yang, C. Q. (2001a). IR spectroscopy study of cyclic anhydride as intermediate for ester crosslinking of cotton cellulose by polycarboxylic acids. V. Comparison of 1,2,4-butanetricarboxylic acid and 1,2,3-propanetricarboxylic acid. *Journal of Applied Polymer Science*, 81, 2142–2150. <https://doi.org/10.1002/app.1650>
- Mao, Z., & Yang, C. Q. (2001b). Polymeric multifunctional carboxylic acids as crosslinking agents for cotton cellulose: Poly(itaconic acid) and in situ polymerization of itaconic acid. *Journal of Applied Polymer Science*, 79, 319–326. [https://doi.org/10.1002/1097-4628\(20010110\)79:2<319::AID-APP140>3.0.CO;2-V](https://doi.org/10.1002/1097-4628(20010110)79:2<319::AID-APP140>3.0.CO;2-V)
- Markoulides, M. S., & Regan, A. C. (2012). Synthesis of a phosphinate analogue of the anti-tumour phosphate di-ester perifosine via sequential radical processes. *Organic & Biomolecular Chemistry*, 11, 119–129. <https://doi.org/10.1039/C2OB26395E>
- Moedritzer, K. (1967). pH dependence of phosphorus-31 chemical shifts and coupling constants of some oxyacids of phosphorus. *Inorganic Chemistry*, 6, 936–939. <https://doi.org/10.1021/ic50051a017>
- Montchamp, J.-L. (2005). Recent advances in phosphorus–carbon bond formation: Synthesis of H-phosphinic acid derivatives from hypophosphorous compounds. *Journal of Organometallic Chemistry*, 690, 2388–2406. <https://doi.org/10.1016/j.jorganchem.2004.10.005>
- Montchamp, J.-L. (2014). Phosphinate chemistry in the 21st century: A viable alternative to the use of phosphorus Trichloride in organophosphorus synthesis. *Accounts of Chemical Research*, 47, 77–87. <https://doi.org/10.1021/ar400071v>
- Mozdyniewicz, D. J., Nieminen, K., Kraft, G., & Sixta, H. (2016). Degradation of viscose fibers during acidic treatment. *Cellulose*, 23, 213–229. <https://doi.org/10.1007/s10570-015-0796-7>
- O'Brien, R. D. (2013). *Toxic phosphorus esters: Chemistry, metabolism, and biological effects*. Elsevier.
- Ortial, S., Fisher, H. C., & Montchamp, J.-L. (2013). Hydrophosphinylation of Unactivated terminal alkenes catalyzed by nickel chloride. *The Journal of Organic Chemistry*, 78, 6599–6608. <https://doi.org/10.1021/jo4008749>
- Parsons, A., & Wright, A. (2008). Synthesis of Bispyrrolidines by radical cyclisation of Diallyl amines using phosphorus hydrides. *Synlett*, 2008, 2142–2146. <https://doi.org/10.1055/s-2008-1072789>
- Peng, H., Yang, C. Q., & Wang, S. (2012). Nonformaldehyde durable press finishing of cotton fabrics using the combination of maleic acid and sodium hypophosphite. *Carbohydrate Polymers*, 87, 491–499. <https://doi.org/10.1016/j.carbpol.2011.08.013>
- Peng, H., Yang, C. Q., Wang, X., & Wang, S. (2012). The combination of Itaconic acid and sodium hypophosphite as a new cross-linking system for cotton. *Industrial and Engineering Chemistry Research*, 51, 11301–11311. <https://doi.org/10.1021/ie3005644>
- Platten, A. W. J., Borys, A. M., & Hevia, E. (2022). Hydrophosphinylation of Styrenes catalysed by well-defined s-block Bimetallics. *ChemCatChem*, 14, Article e202101853. <https://doi.org/10.1002/cctc.202101853>
- Pothast, A., Radosta, S., Saake, B., et al. (2015). Comparison testing of methods for gel permeation chromatography of cellulose: Coming closer to a standard protocol. *Cellulose*, 22, 1591–1613. <https://doi.org/10.1007/s10570-015-0586-2>
- Siller, M., Ahn, K., Pircher, N., et al. (2014). Dissolution of rayon fibers for size exclusion chromatography: A challenge. *Cellulose*, 21, 3291–3301. <https://doi.org/10.1007/s10570-014-0356-6>
- Sivik MR, Gardner RR, Scheper WM (2007) Process for the manufacture of polycarboxylic acids using phosphorous containing reducing agents.
- Sulaeva, I., Budischowsky, D., Rahikainen, J., et al. (2024). A novel approach to analyze the impact of lytic polysaccharide monoxygenases (LPMOs) on cellulosic fibres. *Carbohydrate Polymers*, 328, Article 121696. <https://doi.org/10.1016/j.carbpol.2023.121696>
- Viveros-Ceballos, J., Ordóñez, M., Sayago, F., & Cativiela, C. (2016). Stereoselective synthesis of  $\alpha$ -amino-C-phosphinic acids and derivatives. *Molecules*, 21, 1141. <https://doi.org/10.3390/molecules21091141>
- Wang, J., Fang, K., Liu, X., et al. (2023). A review on the status of formaldehyde-free anti-wrinkle cross-linking agents for cotton fabrics: Mechanisms and applications. *Industrial Crops and Products*, 200, Article 116831. <https://doi.org/10.1016/j.indcrop.2023.116831>
- Wang, J., Xie, M., Liu, X., & Xu, S. (2017). Synthesis of high purity nonsymmetric Diallylphosphinic acid Extractants. *Journal of Visualized Experiments*, 56156. <https://doi.org/10.3791/56156>
- Yang, C. Q. (1993). Infrared spectroscopy studies of the cyclic anhydride as the intermediate for the ester crosslinking of cotton cellulose by polycarboxylic acids. I. Identification of the cyclic anhydride intermediate. *Journal of Polymer Science Part A: Polymer Chemistry*, 31, 1187–1193. <https://doi.org/10.1002/pola.1993.080310514>
- Yang, C. Q., Chen, D., Guan, J., & He, Q. (2010). Cross-linking cotton cellulose by the combination of maleic acid and sodium hypophosphite. 1. Fabric wrinkle resistance. *Industrial and Engineering Chemistry Research*, 49, 8325–8332. <https://doi.org/10.1021/ie1007294>
- Yang, C. Q., He, Q., & Voncina, B. (2011). Cross-linking cotton cellulose by the combination of maleic acid and sodium hypophosphite. 2. Fabric fire performance. *Industrial and Engineering Chemistry Research*, 50, 5889–5897. <https://doi.org/10.1021/ie1022892>
- Yao, W., Wang, B., Ye, T., & Yang, Y. (2013). Durable press finishing of cotton fabrics with citric acid: Enhancement of whiteness and wrinkle recovery by polyol extenders. *Industrial and Engineering Chemistry Research*, 52, 16118–16127. <https://doi.org/10.1021/ie402747x>
- Zhao, C., & Sun, G. (2015). Catalytic actions of sodium salts in direct esterification of 3,3',4',4'-benzophenone Tetracarboxylic acid with cellulose. *Industrial and Engineering Chemistry Research*, 54, 10553–10559. <https://doi.org/10.1021/acs.iecr.5b02308>
- Zhu, P., & Liu, J. (2018). Preparation and properties of cross-linked regenerated cellulose fibers. *J Textile Sci Eng*, 08. <https://doi.org/10.4172/2165-8064.1000354>